Supporting Information — Dynamic Permeability in Metastable Droplet Interfacial Bilayers

Nivedina A. Sarma,[1,2,*] David A. King,[1,2,*] Xuefei Wu,[2] Brett A. Helms,[3,2] Paul D. Ashby,[3,2] Thomas P. Russell,[4,2] and Ahmad K. Omar[1,2,†]

[1]*Department of Materials Science and Engineering, University of California, Berkeley, California 94720, USA*
[2]*Materials Sciences Division, Lawrence Berkeley National Laboratory, Berkeley, California, 94720, USA*[*]
[3]*The Molecular Foundry, Lawrence Berkeley National Laboratory, Berkeley, California, 94720, USA*
[4]*Polymer Science and Engineering Department, University of Massachusetts, Amherst 01003, USA*

FINITE NORMAL STRESS DIFFERENCE NEAR PORE RADIUS

We show how, by assuming that the normal stress difference is sharply peaked at the pore interface, the jump in the radial across is the interface is related to line tension as in Eq. (10). First, we know from Eq. (10) of the main text

$$\frac{\partial \Sigma_{rr}}{\partial r} = \frac{2}{r}\left(\Sigma_{rr} - \Sigma_{tt}\right). \tag{S1}$$

Integrating both sides from $R^\dagger_-$ (inside the pore) to $R^\dagger_+$ (outside the pore) we obtain

$$\Sigma_{rr}(R^\dagger_+) - \Sigma_{rr}(R^\dagger_-) = \int_{R^\dagger_-}^{R^\dagger_+} dr\, \frac{2}{r}\left(\Sigma_{rr} - \Sigma_{tt}\right). \tag{S2}$$

In a spatially uniform system, the normal stress difference must vanish. Close to the pore interface, however, there is a sudden change in composition that results in the normal stress difference being sharply peaked around $R^\dagger$. This allows the integral to be approximated following Ref. [78] by Taylor expanding $1/r$ about that radius, and truncating at desired order:

$$\int_{R^\dagger_-}^{R^\dagger_+} dr\, \frac{2}{r}\left(\Sigma_{rr} - \Sigma_{tt}\right) = \frac{1}{R^\dagger}\sum_{n=0}^{\infty}(-1)^n (R^\dagger)^{-n} \int_{R^\dagger_-}^{R^\dagger_+} dr\, (r - R^\dagger)^n \left(\Sigma_{rr} - \Sigma_{tt}\right). \tag{S3}$$

If we discard those terms $\mathcal{O}((R^\dagger)^{-2})$ and greater, we obtain the result in the main text:

$$\Sigma_{rr}(R^\dagger_+) - \Sigma_{rr}(R^\dagger_-) = \frac{2}{R^\dagger}\sigma + \mathcal{O}((R^\dagger)^{-2}), \tag{S4}$$

where the line tension is defined as

$$\sigma = \int_{R^\dagger_-}^{R^\dagger_+} dr\, \left(\Sigma_{rr} - \Sigma_{tt}\right). \tag{S5}$$

LINEARIZATION OF IN-PLANE SURFACTANT DYNAMICS

Here we demonstrate, through linearizing the equations of motion for the membrane composition, that the composition current is directly proportional to the gradient in the effective surface tension [as in Eq. (16)] and that, in steady state, the effective surface tension solves the Laplace equation [see Eq. (17)].

We begin with the continuity equation

$$\frac{\partial \phi}{\partial t} = -\nabla\cdot\mathbf{j} = -\nabla\cdot\left(M(\phi)\nabla\cdot\boldsymbol{\Sigma}\right), \tag{S6}$$

where the concentration dependence of the mobility, M, has been made explicit. We suppose that the composition varies weakly around the uniform value ϕ_0^{mem}, so that $\phi \approx \phi_0^{\mathrm{mem}} + \delta\phi$. By weakly varying, we suppose that $1 \gg |\nabla\delta\phi| \gg \nabla^2\delta\phi \gg (\cdots)$ so that only the lowest derivatives of $\delta\phi$ need to be kept to leading order. This assumption greatly simplifies the stress tensor since, from Eq. (6) of the main text, all terms other than the effective surface tension include derivatives of $\delta\phi$. It follows from this assumption that $\boldsymbol{\Sigma} \approx \gamma_{\mathrm{eff}}\mathbf{I}$. To this order, the continuity equation is then written:

$$\frac{\partial \phi}{\partial t} = -\nabla\cdot\left(M(\phi)\nabla\gamma_{\mathrm{eff}}\right). \tag{S7}$$

Expanding the divergence on the right-hand side, we obtain $\nabla M(\phi)\cdot\nabla\gamma_{\rm eff} + M(\phi)\nabla^2\gamma_{\rm eff}$. The first term is necessarily $\mathcal{O}(|\nabla\delta\phi|^2)$, while the lowest order contribution to the second is $M(\phi_0^{\rm mem})\nabla^2\gamma_{\rm eff}$. If we define the constant single-particle mobility in a uniform composition membrane as $M(\phi_0^{\rm mem}) = M_0$, the continuity equation becomes, to leading order,

$$\frac{\partial\phi}{\partial t} \approx -M(\phi_0^{\rm mem})\nabla^2\gamma_{\rm eff}. \tag{S8}$$

Thus, if we neglect time-variations in the composition, the effective tension is *harmonic*; $\nabla^2\gamma_{\rm eff} = 0$. Furthermore, we may extract the approximate current, *post hoc*, $\mathbf{j} \approx M_0\nabla\gamma_{\rm eff}$ as in Eq. (16) of the main text.

DETAILS OF UNIVERSAL SCALING FUNCTION

We show that, under the assumptions that the bilayer size far exceeds any of the pores and that the system has reached the self-similar, stable, long-time distribution given by Eq. (22), we obtain *the same* universal scaling function as in the LSW theory. We also present some details of how to arrive at its form.

To derive the scaling function $\mathcal{N}(x)$, we begin with the continuity equation (absent a generation term):

$$\frac{\partial n}{\partial t} + \frac{\partial}{\partial R}(v(R)n) = 0 \tag{S9}$$

and use the relevant interface velocity and self-similarity ansatz $n(R,t) = \mathcal{N}(x)/R_c^{-(d+1)}$ where $x = R/R_c$. For the Ostwald ripening mechanism, Eq. (S9) becomes:

$$\begin{aligned}
&\frac{\partial}{\partial t}(R_c^{-(d+1)}\mathcal{N}(x)) + \frac{\partial}{\partial R}\left(\frac{2M_0\sigma}{R^2\ln(\ell/R)}\left(\frac{R}{R_c}-1\right)\right)(R_c^{-(d+1)}\mathcal{N}(x)) \\
&R_c^{-(d+2)}\dot{R}_c[(d+1)\mathcal{N}(x) + x\mathcal{N}'(x)] = \frac{1}{R_c^3 R_c^{-(d+1)}}\frac{1}{\ln(R_c/\ell)}\frac{\partial}{\partial x}\left(\frac{2M_0\sigma}{x}\left(1-\frac{1}{x}\right)\mathcal{N}(x)\right) \\
&-R_c^2\ln(R_c/\ell)\dot{R}_c = \frac{2M_0\sigma\dfrac{\partial}{\partial x}\left(\dfrac{1}{x}-\dfrac{1}{x^2}\right)\mathcal{N}(x)}{[(d+1)\mathcal{N}(x) + x\mathcal{N}'(x)]} = \varepsilon.
\end{aligned} \tag{S10}$$

We note that since $R_c \ll \ell$, the logarithmic term in the denominator of the penultimate line is large and negative. Furthermore, it varies logarithmically with R_c and thus much more slowly than the algebraic terms R_c^2 and R_c^{-3}. We therefore treat $\ln R_c/\ell$ as quasi-static and extract it from the derivative to make the problem analytically tractable. Multiplying both sides by $R_c^2\ln R_c/\ell$ provides the final line, where we have grouped those terms that depend on R_c and $\mathcal{N}(x)$ on the left and right sides of the equation, respectively. Since the LHS of Eq. (S10) depends on time through R_c and the RHS depends only on x, both sides must be equal to a constant that is independent of both x and t.

We can solve for $\mathcal{N}(x)$ and identify ε by decomposing the integrand $\ln\mathcal{N}(x)$ into partial fractions and finding the roots of the denominator:

$$\ln\mathcal{N}(x) = \int^x \frac{\mathcal{N}'(x)}{\mathcal{N}(x)}dx = \int^x \frac{dy}{y}\frac{(-\varepsilon(d+1)y^3 + 2 - y)}{(\varepsilon y^3 - y + 1)}. \tag{S11}$$

The polynomial in the denominator of Eq. (S11) is a depressed cubic because it does not have a y^2 term. One may apply Cardano's formula, which states that for a depressed cubic polynomial with the form $ay^3 + by + c$, the discriminant is $\mathcal{D} = -4b^3a - 27a^2c^2$. Applying the coefficients for the depressed cubic in Eq. (S11) gives

$$\mathcal{D} = -4(-1)\varepsilon - 27\varepsilon^2(1). \tag{S12}$$

Because x is a ratio of length scales, we know the roots of the denominator in Eq. (S11) must be positive and real. This restricts $\mathcal{D} \geq 0$, which in turn results in $\varepsilon \leq 0$. When $\varepsilon = 4/27, \mathcal{D} = 0$ and the polynomial has a repeated real root. If $\varepsilon < 4/27, \mathcal{D} > 0$ and the polynomial has three distinct real roots. LSW argue that $\varepsilon = 4/27$ is the only stable solution to the problem [47]. We proceed

with this value of ε to find the full form of $\mathcal{N}(x)$:

$$\ln\mathcal{N}(x) = \int^x dy \frac{(-\varepsilon(d+1)y^3+2-y)}{y(\varepsilon y^3-y+1)} = \int^x dy \frac{2-y-(4/27)(d+1)y^3}{y\left((4/27)y^3-y+1\right)} = \int^x dy \frac{54-27y-4(d+1)y^3}{4y\left(y-(3/2)\right)^2(y+3)}$$

$$= \int^x dy \frac{A}{y} + \frac{B}{y-(3/2)} + \frac{C}{\left(y-(3/2)\right)^2} + \frac{D}{y+3}, \tag{S13}$$

$$\text{where } 54-27y-4(d+1)y^3 = 4A\left(y-\frac{3}{2}\right)^2(y+3) + 4By\left(y-\frac{3}{2}\right)(y+3) + 4Cy(y+3) + 4Dy\left(y-\frac{3}{2}\right)^2.$$

We solve for each of A, B, C and D by setting y to the value that takes the denominator to 0 (i. e. $y = 0$ to solve for A, $y = 3/2$ to solve for C, $y = -3$ to solve for D). We then integrate and exponentiate Eq. (S13) to obtain

$$\mathcal{N}(x) = \mathcal{C}x^2\left(\frac{3}{2}-x\right)^{-\left(2+\frac{5d}{9}\right)}(3+x)^{-\left(1+\frac{4d}{9}\right)}\exp\left(-\frac{d}{3-2x}\right), \tag{S14}$$

which is general to any dimension. We use the $d = 2$ case to find results for Ostwald ripening on 2-dimensional membrane systems.

DERIVING THE TIMESCALE OF GROWTH THROUGH DESORPTION

In this appendix, we discuss the pore growth dynamics in the case that growth is driven purely by desorption of surfactants from the pore perimeter. We determine how the pore size distribution evolves with time and how this affects the dynamic permeability of the membrane. Our starting assumption is that surfactant exclusively desorbs from the perimeter of the pore at a constant rate rate ω, such that the radial velocity of the pore is

$$v(R) = 2\pi\omega R. \tag{S15}$$

This form of the velocity shows that the radial growth rate is proportional to the pore perimeter.

We shall suppose that the initial distribution of pore radii is known, which allows us to determine the pore-size distribution per unit area, $n(R,t)$, from the continuity equation:

$$\frac{\partial}{\partial t}n(R,t) + \frac{\partial}{\partial R}[v(R)n(R,t)] = 0. \tag{S16}$$

Note that there is no source term here, $\mathcal{C} = 0$ in Eq. (11). This is because, in the absence of mechanisms such as coalescence, desorption only changes the pore size continuously. Furthermore, in contrast to growth mechanisms such as Ostwald ripening and coalescence, in which the number density n decreases as smaller pores shrink or pores merge together, desorption-driven growth conserves the number of pores. As the pores grow larger, the total pore area increases, making the area fraction and number density proportional to one another.

Equation (S16) is a linear first-order PDE in $n(R,t)$, which may be solved exactly. To simplify our analysis, we define

$$y(R,t) = v(R)n(R,t), \tag{S17}$$

so that Eq. (S16) becomes

$$\frac{\partial y}{\partial t} + v(R)\frac{\partial y}{\partial R} = 0. \tag{S18}$$

Now we make a change of variables from (t,R) to (s,x) defined through

$$s(t,R) = t, \tag{S19a}$$

$$x(t,R) = t + f(R). \tag{S19b}$$

The chain rule then gives us

$$\frac{\partial y}{\partial t} = \frac{\partial y}{\partial s} + \frac{\partial y}{\partial x} \tag{S20a}$$

$$\frac{\partial y}{\partial R} = f'(R)\frac{\partial y}{\partial x}. \tag{S20b}$$

These allow us to write Eq. S16 as

$$\frac{\partial y}{\partial s} + \frac{\partial y}{\partial x} + v(R)f'(R)\frac{\partial y}{\partial x} = 0. \tag{S21}$$

If we choose $f'(R) = -1/v(R)$, then the final two terms of the above equation cancel, leaving

$$\frac{\partial y}{\partial s} = 0. \tag{S22}$$

Therefore, y is a function of x *only*. Recalling our choice of $f(R) = -\int^R dR'/v(R')$ we have

$$y(R,t) = Y(x) = Y\left(t - \int^R \frac{dR'}{v(R')}\right). \tag{S23}$$

We evaluate Eq. (S23) using the velocity defined in Eq. (S17):

$$\int^R \frac{dR'}{v(R')} = \int^R \frac{dR'}{2\pi\omega R'} = \frac{1}{2\pi\omega}\log R. \tag{S24}$$

Defining $\tau = (2\pi\omega)^{-1}$ yields

$$\begin{aligned} x &= t/\tau - \log R, \\ y(R,t) &= Y(t/\tau - \log R), \end{aligned} \tag{S25}$$

which implies

$$n(R,t) = \frac{1}{2\pi\omega R}Y(t/\tau - \log R). \tag{S26}$$

Given an initial distribution $n(R, t = 0) = n_0(R)$, we find Y by solving

$$n_0(R) = \frac{1}{2\pi\omega R}Y(-\log R). \tag{S27}$$

Let us suppose that the initial distribution is Gaussian with mean $\overline{R}_0$ and standard deviation σ then,

$$n_0(R) = \frac{2\sigma^2}{1 + \mathrm{erf}\left(\sigma\overline{R}_0/2\right)}\frac{1}{\sqrt{2\pi}\sigma}\exp\left(-\frac{(R-\overline{R}_0)^2}{2\sigma^2}\right). \tag{S28}$$

Note the somewhat complicated normalisation constant. The distribution is only defined on the interval $R \in [0, \infty]$, since pores cannot have negative radii, so the distribution must satisfy $\int_0^\infty dR n_0(R) = 1$. We find

$$Y(-\log R) = \frac{2\sigma^2}{1 + \mathrm{erf}\left(\sigma\overline{R}_0/2\right)}\frac{2\pi\omega R}{\sqrt{2\pi}\sigma}\exp\left(-\frac{(R-\overline{R}_0)^2}{2\sigma^2}\right), \tag{S29}$$

from which we obtain

$$\begin{aligned} n(R,t) &= \frac{2\sigma^2}{1 + \mathrm{erf}\left(\sigma\overline{R}_0/2\right)}\frac{1}{\sqrt{2\pi}\sigma(t)}\exp\left(-\frac{(R-\overline{R}(t))^2}{2\sigma(t)^2}\right) \\ \overline{R}(t) &= \overline{R}_0 e^{t/\tau} \\ \sigma(t) &= \sigma e^{t/\tau}. \end{aligned} \tag{S30}$$

This shows that, up to modifications due to the one-sided nature of the distribution, an initially Gaussian $n(R,t)$ remains so as the pores grow but *both* the mean and variance increase exponentially with e-folding time τ.

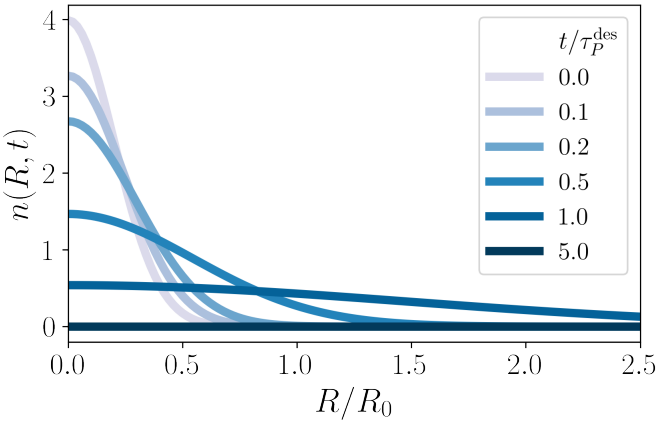

FIG. S1. Pore distribution for the desorption mechanism, plotted as a function of the pore size relative to the initial pore radius, R/R_0, for various different times in units of the characteristic desorption time, $t/\tau_P^{\rm des}$.

Figure S1 shows how the pore size distribution evolves in the desorption mechanism. The distribution remains Gaussian with a mean and variance that grow exponentially with time

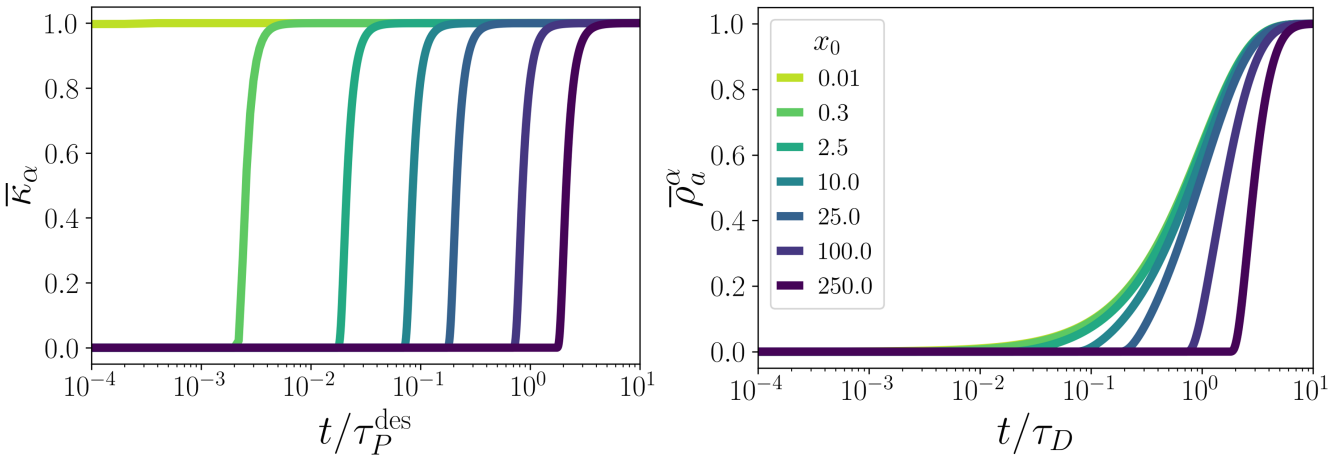

FIG. S2. Evolution under the desorption mechanism of: the dimensionless membrane permeability, $\overline{\kappa}^\alpha$ as a function of time relative to the desorption time scale $t/\tau_P^{\rm des}$ (left) and the dimensionless acceptor density as a function of time relative to the dye diffusion time scale t/τ_D (right).

Figure S2 shows the dynamic membrane permeability and the density change in the acceptor droplet for particles of various sizes. In contrast to the Ostwald ripening results presented in Figs. 4 and 5 in the main text, the desorption mechanism seems particles of vastly different sizes cross the membrane at roughly the same time. This is an indication that for highly size-selective systems, pore growth likely occurs through Ostwald ripening.

We consider the rate at which particles must desorb to allow for size-selectivity comparable to the cases in which pores growth with algebraic scaling. In order for particles of size r_1 and $2r_1$ to cross the bilayer one order of magnitude part so that $t_{50}^{(r_1)} = 10t_{50}^{(2r_1)}$, we know from Eq. (S30) that

$$\begin{aligned} R_0 \exp\left[2\pi\omega t_{50}^{(r_1)}\right] &= r_1 \\ R_0 \exp\left[2\pi\omega t_{50}^{(2r_1)}\right] &= 2r_1 \\ 2 = \exp\left[2\pi\omega\left(t_{50}^{(2r_1)} - t_{50}^{(r_1)}\right)\right] &= \exp\left[18\pi\omega t_{50}^{(r_1)}\right]. \end{aligned} \tag{S31}$$

In the case that $t_{50}^{(r_1)} = 1$ hour, $\omega = 10^{-2}$ particles per hour, which corresponds to 1 surfactant desorbing from the membrane

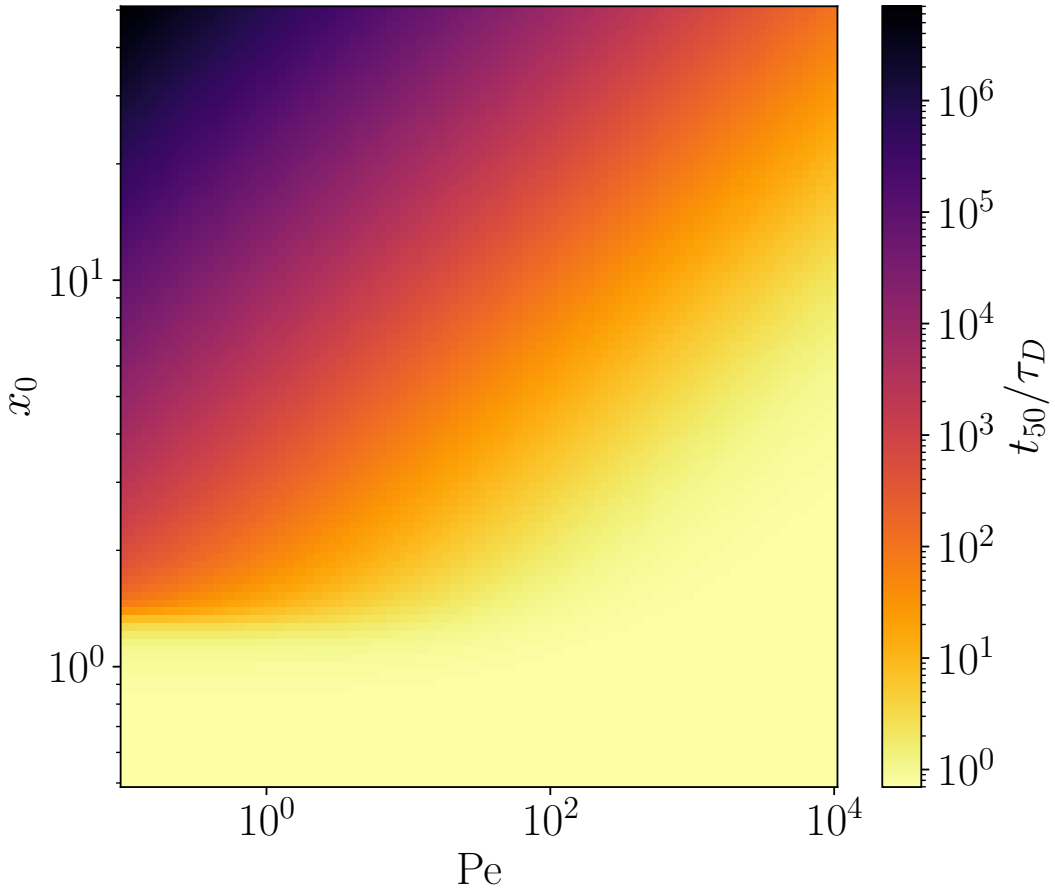

FIG. S3. Full contour map for t_{50}/τ_D for the Ostwald ripening mechanism. We see that the time for half the particles of a given size to enter the acceptor droplet plateaus to $\ln 2$ for $x_0 < 3/2$ and for increasing Pe. The transition to this plateau becomes steeper as Pe decreases.

every 100 hours. In the case that $t_{50}^{(r_1)} = 1$ day, $\omega = 10^{-2}$ particles per day, which corresponds to 1 surfactant desorbing from the membrane every 100 days. This implies that, any appreciable amount of desorption will lead to extremely rapid transport of dye of essentially any size. Therefore, desorption is unlikely to be the mechanism of pore growth in DIBs that prevent particles crossing for any extended period of time.

CONTOUR MAP FOR OSTWALD RIPENING

Here, we provide the full contour map for t_{50}/τ_D in the Ostwald ripening mechanism across three decades of particle size and five decades of Pe. The time for 50% of a particular species to enter the acceptor plateaus to $\ln 2$ at low x_0 and large Pe. The transition to that plateau is steepest at low Pe, for which t_{50}/τ_D dramatically drops to $\ln 2$ for the particles that fit through the pores present in the initial distribution ($x_0 < 3/2$). As Pe increases, the plateau becomes smoother and occurs at larger x_0. The figure provided in the main text is made from taking vertical and horizontal slices from this plot to observe how t_{50}/τ_D varies with x_0 for constant Pe and with Pe for constant x_0, respectively.

* These authors contributed equally to this work
† aomar@berkeley.edu